



Article  
scientifique

Revue de la  
littérature

2018

Accepted  
version

Public  
access

This is an author manuscript post-peer-reviewing (accepted version) of the original publication. The layout of the published version may differ .

---

New developments and possibilities of wide-pore superficially porous particle technology applied for the liquid chromatographic analysis of therapeutic proteins

---

Bobaly, Balazs; Veuthey, Jean-Luc; Guillarme, Davy; Fekete, Szabolcs

#### How to cite

BOBALY, Balazs et al. New developments and possibilities of wide-pore superficially porous particle technology applied for the liquid chromatographic analysis of therapeutic proteins. In: Journal of Pharmaceutical and Biomedical Analysis, 2018, vol. 158, p. 225–235. doi: 10.1016/j.jpba.2018.06.006

This publication URL: <https://archive-ouverte.unige.ch/unige:106641>

Publication DOI: [10.1016/j.jpba.2018.06.006](https://doi.org/10.1016/j.jpba.2018.06.006)

© This document is protected by copyright. Please refer to copyright holder(s) for terms of use.

Last deposit update in Archive ouverte UNIGE on 15.03.2023 09:27

1           **New developments and possibilities of wide-pore superficially porous particle**  
2           **technology applied for the liquid chromatographic analysis of therapeutic proteins**

3  
4  
5           Balázs Bobály, Jean-Luc Veuthey, Davy Guillarme, Szabolcs Fekete\*

6  
7  
8           <sup>a</sup> School of Pharmaceutical Sciences, University of Geneva, University of Lausanne, Rue  
9           Michel Servet, 1, 1206 Geneva 4, Switzerland

10  
11           **CORRESPONDENCE:** Szabolcs Fekete

12           Phone: +41 22 37 963 34

13           Fax: +41 22 379 68 08

14           E-mail: [szabolcs.fekete@unige.ch](mailto:szabolcs.fekete@unige.ch)

15

16           **New developments and possibilities of wide-pore superficially porous particle**  
17           **technology applied for the liquid chromatographic analysis of therapeutic proteins**

18  
19  
20   **Abstract**

21   This review paper discusses about the success of columns packed with superficially porous  
22   particles (SPP) in liquid chromatography for the analysis of peptides and proteins. First, it  
23   summarizes the history of SPP, including the development of different SPP generations from  
24   particles of 50  $\mu\text{m}$  to sub-2  $\mu\text{m}$ . It also critically discusses the improved kinetic performance of  
25   SPP particles in comparison to fully porous particles. The current trends and applications of  
26   columns packed with SPPs for the analysis of peptides and proteins (including mAbs and ADC  
27   at the intact and sub-unit levels) are shown, as well. Finally, some of the potential perspectives  
28   for this technology are also described, including the radially oriented mesopores or the  
29   applicability of the technology for chiral separations.

30  
31   **Keywords:**

32   Superficially porous particles, core-shell, wide-pore, protein, monoclonal antibody, antibody-  
33   drug-conjugate

## 36 **1. History of columns packed with SPP particles**

37 In the recent development of particle technology targeted for liquid chromatography (LC), the  
38 use of superficially porous (SPP or often called as shell, core-shell, fused-core or partially-  
39 porous) particles has received considerable attention [1,2]. SPPs manifest the advantages of  
40 porous and nonporous particles. Knox was the first to recommend the use of thin films of the  
41 stationary liquid phase in liquid–liquid chromatography [3]. The concept of superficial stationary  
42 phases in LC, was first introduced Horváth and co-workers in the late 1960s [4,5]. Horváth  
43 applied 50  $\mu\text{m}$  glass bead particles covered with styrene-divinylbenzene based ion exchange  
44 resin, known as pellicular packing material for the separation of nucleotides. Later, Kirkland  
45 showed, that 30–40  $\mu\text{m}$  diameter SPPs provide much faster separations, compared to the  
46 large porous particles used earlier in LC [6]. The motivation behind the development of such  
47 materials was that columns packed with partially porous particles would have a higher  
48 efficiency than those packed with fully porous particles, because diffusion through the thin  
49 porous layer surrounding the particles would be faster than diffusion through the whole  
50 particles [2]. This acceleration of diffusion would reduce the time required for solute  
51 equilibration between the porous layer and the mobile phase or, more exactly, would effectively  
52 reduce the resistance to mass transfer through the stationary phase [2]. This feature should  
53 be especially beneficial for the separation of large molecules possessing low diffusivity. This  
54 idea made sense at a time when the average particle sizes were ca. 80  $\mu\text{m}$ . Therefore 30-50  
55  $\mu\text{m}$  particles with very thin porous shell have been commercialized in the 1970s under different  
56 brand names such as Zipax, Corasil and Pellicosil [6,7,8].

57 In the 1990s, non-porous particles have also been considered as a valuable option for protein  
58 separations. Issaeva *et al.* showed an extremely high speed separation of proteins and  
59 peptides using 1.5  $\mu\text{m}$  non-porous particles (Micra) [9]. Barder *et al.* also demonstrated that  
60 the efficiency of columns packed with non-porous silica particles was considerably higher than  
61 that of columns packed with porous particles, especially at high flow-rates [10]. Non-porous  
62 particles can indeed provide lower mass transfer resistance and higher efficiency than porous  
63 particles, but they are suffering from a lower specific volume and sample loading capacity.  
64 Seifar *et al.* estimated a 50-fold higher sample capacity for porous particles compared to non-  
65 porous particles of the same size [11]. In another work, the loading capacity for the 1.7  $\mu\text{m}$  fully  
66 porous Acquity C18 particles was found to be 16 times larger than for non-porous 1.5  $\mu\text{m}$   
67 particles [12]. Another issue related to the use of non-porous particles is its very low retention  
68 capacity compared to fully porous ones. It was shown that the average carbon load for 1.5  $\mu\text{m}$   
69 non-porous particles was about 56 times lower than for 1.7  $\mu\text{m}$  Acquity C18 porous particles  
70 [12]. The lower carbon load provides a lower phase ratio for non-porous particles, which leads  
71 to significantly lower retention. Due to the above mentioned limitations, non-porous materials  
72 never had too much success.

73 SPP materials had had a regain interest in the year 2000 and the second generation of SPPs  
74 then appeared [13]. At this time, the commercial 5  $\mu\text{m}$  particles, having an average pore size  
75 of 300  $\text{\AA}$  and 0.25  $\mu\text{m}$  shell thickness (it was called Poroshell), showed excellent efficiency for  
76 macromolecule separations. Few years later a new generation of SPPs has been developed  
77 and particles having standard-pores (90 and 100  $\text{\AA}$ ) were successfully applied for small  
78 molecules separations. These were the so-called sub-3  $\mu\text{m}$  SPPs and their structure was very  
79 close to the optimum morphology, offering a good compromise between column efficiency and  
80 loadability. They were commercialized under the brand names of Halo, Ascentis Express and  
81 Kinetex [14,15,16]. A sub-3  $\mu\text{m}$  particle with the pore size of 160  $\text{\AA}$  packing was introduced in  
82 2010 by Advanced Material Technology (AMT) and Supelco under the brand names of Halo  
83 Peptide ES-C18 and Ascentis Express Peptide ES-C18, respectively [17,18]. An average pore  
84 size of 160  $\text{\AA}$  allowed the unrestricted access of molecules up to approximately 15 kDa,  
85 depending on the molecular conformation [19]. Kirkland *et al.* compared the efficiency of the  
86 160  $\text{\AA}$  and 90  $\text{\AA}$  SPPs for mixtures of peptides and small proteins [18]. Small proteins (i.e.,  
87 ribonuclease, insulin, cytochrome C and lysozyme) exhibited broadened peaks with the 90  $\text{\AA}$   
88 SPP, indicating restricted diffusion, but they eluted in narrow peaks from the 160  $\text{\AA}$  SPP  
89 column.

90 In 2012, a larger (3.6  $\mu\text{m}$ ) SPP wide-pore material (0.2  $\mu\text{m}$  shell thickness) was launched under  
91 the name Aeris Widepore, and seemed to be particularly promising for large protein  
92 separations including monoclonal antibody (mAb) fragments [20,21]. Its relatively large particle  
93 diameter afforded low column pressures, which could help to minimize potential on-column  
94 degradation of pressure sensitive proteins, by avoiding high shear forces, and to minimize  
95 pressure induced increases in hydrophobic retention that can contribute to peak broadening  
96 [22,23]. To analyse intact large proteins and their sub-units, the particle size and shell  
97 thickness were further optimized [24]. Both theory and previous experimental studies indicated  
98 that a thin shell should be used to compensate for the low diffusion coefficients of large  
99 molecules. To find the optimum particle morphology, three different batches of 3.4  $\mu\text{m}$  particles  
100 with 400  $\text{\AA}$  pores and thick shells of 0.15, 0.20 or 0.25  $\mu\text{m}$  were compared in an experimental  
101 study [24]. It was found that a 0.20  $\mu\text{m}$  shell thickness (400  $\text{\AA}$ ) provided the highest  
102 chromatographic performance for proteins. This material is now commercially available under  
103 the brand name HALO Protein. It was found that the larger pore size actually had more impact  
104 on the kinetic performance achieved with mAbs, than the particle size and shell thickness. The  
105 SPPs with larger particle size (3.5  $\mu\text{m}$ ) and pore size (450  $\text{\AA}$ ) showed the highest resolution  
106 for mAbs [25]. This results led to the optimal particle design with a particle size of 3.5  $\mu\text{m}$ , a  
107 thin shell of 0.25  $\mu\text{m}$  and pore size of 450  $\text{\AA}$ . This material is now commercialized as  
108 AdvanceBio RP-mAb. Later, SPPs with 1000  $\text{\AA}$  pores designed specifically for separating large  
109 biomolecules and industrial polymers have been described and showed benefits compared to

110 300-400 Å SPPs [26]. Very recently, another wide-pore silica-based SPP with a high coverage  
111 phenyl bonding has been released and successfully applied for the analysis of mAbs and  
112 antibody-drug conjugates (ADCs) [27]. This new material (BioResolve RP mAb polyphenyl) is  
113 based on 2.7 µm particles having a shell thickness of 0.40 µm and average pore size of  
114 approximately 450 Å.

115 As shown, there is still a continuous development in SPP technology and more and more  
116 efficient stationary phases are regularly released. Various particle morphologies (i.e. particle  
117 size, shell thickness, pore size) are now available for protein separations, and figure 1  
118 illustrates the history of SPP development. The aim of this paper is to review the latest  
119 developments and applications of wide-pore SPPs applied for large molecule separations and  
120 provide some guidelines for method development. Some future perspectives are also  
121 presented.

122

## 123 **2. Advantages of SPP technology**

124 The peak dispersion in chromatography is generally characterized by the theoretical plate  
125 height ( $H$ ) and the number of theoretical plates ( $N$ ). The treatment of mass transfer processes  
126 and the distribution equilibrium between the mobile and stationary phase in a column lead to  
127 equations which link the theoretical plate height to the properties of the chromatographic  
128 systems, such as the linear velocity. First, Van Deemter proposed an equation, which  
129 described the column performance as a function of the linear velocity [28]. Since then, several  
130 plate height and rate models were derived for LC, by numerous researchers. Knox suggested  
131 a useful empirical three term equation to describe the dependency of the theoretical plate  
132 height of a column as a function of linear velocity [29]. In this well-known equation, the three  
133 parameters  $A$ ,  $B$ , and  $C$  are determined by the magnitude of band broadening due to eddy  
134 dispersion, longitudinal diffusion, and mass transfer resistance, respectively. The  $A$ -term  
135 depends on the quality of the column packing including: (1) the homogeneity of the packed  
136 bed structure, (2) the arrangement of the particles in the wall and the central regions of the  
137 column and probably (3) on the particle size distribution. The  $B$ - and  $C$ -terms of the plate height  
138 equation depend on analyte retention. The  $B$ -term increases with analyte retention, as more  
139 time is available for diffusion to take place in the stationary phase (surface diffusion). The  $C$ -  
140 term expresses the resistance to mass transfer and can be divided into trans-particle (or intra-  
141 particle) and external- (or film-) mass transfer resistance contributions. It is expected by the  
142 theory that the eddy dispersion contributions to the efficiency of columns packed with SPPs  
143 would correspond to the external diameter of the particle, but the internal mass-transfer  
144 resistances and longitudinal diffusion would correspond to the thickness and pore diameter of  
145 the porous layer. The initial idea of preparing SPPs was to increase the column efficiency by  
146 reducing the mass transfer resistance across the particles. However, it seems that trans-

147 particle mass transfer resistance is far from being the dominant contribution to band  
148 broadening in HPLC [1,2]. Indeed, the columns packed with the new generation of SPPs are  
149 successful, but for other reasons [2].

150 According to the theory, the intra-particle diffusivity depends on the ratio of the solid core  
151 diameter to that of the particle diameter in a SPP. This ratio is often called as *rho* ( $\rho$ ) and used  
152 as a measure of particle morphology of SPPs. As this ratio increases, the mass transfer  
153 kinetics becomes faster through the particles. Similarly, the external mass transfer also  
154 depends on the structure of the particles. According to some recent experimental  
155 measurements, the mass transfer kinetic is mostly accounted for the external film mass  
156 transfer resistance across the thin layer of the mobile phase surrounding the external surface  
157 area of the particles [2]. This suggests that, the initial idea of preparing SPPs with the purpose  
158 to increase column efficiency by reducing the mass transfer resistance across the particles  
159 might provide only modest practical gains for the separation of low or medium molecular weight  
160 compounds [2]. To conclude on the mass transfer resistance, approximately 2 times lower *C*-  
161 term is expected with current SPP than with the same size fully porous particles. The gain in  
162 the *C*-term is more important for large biomolecules and less for small molecules possessing  
163 high diffusivity.

164 On the other hand, the presence of a solid core inside the particles has a direct consequence  
165 on the longitudinal diffusion term (*B*-term), since it decreases this contribution to the plate  
166 height by about 20 % when the ratio of the core to the particle diameter is  $\rho \sim 0.6$  (which is  
167 very common for normal pore SPPs) [1,2]. However, the reduced internal porosity of the SPPs  
168 brings a limited improvement in their efficiency. Experimentally, it was implied that the solid  
169 core reduced the *B*-term by not more than 30 % in comparison to fully porous particles [30].  
170 As a conclusion, it can be stated that recent SPPs manifest a gain of approximately 20-30 %  
171 in the longitudinal diffusion. This causes only a gain of a  $\sim 10$  % increase in the total column  
172 efficiency compared to that of columns packed with fully porous particles. However, we have  
173 to keep in mind that for large molecules (possessing low diffusivity), the *B*-tem contribution is  
174 practically negligible. This benefit is only important for small molecules and for separations  
175 performed at low flow rates (long separations).

176 Finally, according to several experimental results, the eddy dispersion term (*A*-term) of the  
177 columns packed with SPPs is significantly smaller ( $\sim 30$ - $40$  %) than that of the columns packed  
178 with fully porous particles [1,2]. It is surprising, since particle morphology should not affect the  
179 zig-zag multipath dispersion of solutes occurring in the interstitial column volume. It is still  
180 unclear whether this significant improvement in efficiency is due to the narrow particle size  
181 distribution (PSD) of SPPs [31]. Some recent studies have indeed suggested that particles  
182 displaying a very narrow PSD can lead to unprecedented low minimal plate heights [1,2]. It is  
183 however uncertain whether this finding can be purely related, because there are also other

184 factors that might influence the packing quality. Superficially porous particles have indeed a  
185 higher density and some of them are rougher than fully porous particles [32]. This might also  
186 have had an influence on the achieved packing quality, apart from the PSD.

187 To conclude on the efficiency of SPPs, the success of these materials in the separation of  
188 small molecules is not primarily a result of the decrease of the C-term, as it is often claimed in  
189 commercial brochures. Most importantly, the exceptional performance of columns packed with  
190 SPPs is probably caused by the important reduction of the eddy dispersion term. For large  
191 molecules, however the decrease of the C-term is the most important benefit of SPPs.  
192 Theoretically, as the  $\rho$ -value increases (the thinner the porous shell is), significantly lower C  
193 term contribution is expected. This is probably the reason why commercial wide-pore SPP  
194 materials possess higher  $\rho$ -values ( $0.70 < \rho < 0.94$ ) than standard pore SPPs ( $0.62 < \rho < 0.76$ )  
195 [27,33]. On the other hand, wide-pore SPPs possess larger particle diameter ( $2.7 \mu\text{m} \leq d_p \leq 5$   
196  $\mu\text{m}$ ) compared to standard pore ones ( $1.3 \mu\text{m} \leq d_p \leq 5 \mu\text{m}$ ), to avoid very high pressures which  
197 can drastically affect protein separations (retention, degradation, conformation).

198

### 199 **3. Commercially available wide-pore SPPs**

200 Currently available SPPs for proteins and peptides applications are predominantly RPLC  
201 phases, but some SPPs are also available for HILIC peptide applications [34]. RPLC offers the  
202 highest separation efficiency for mAb and related protein separations [35]. Its robustness, ease  
203 of use and possibility to hyphenate with mass spectrometry (MS) made RPLC well suited both  
204 for routine applications and R&D environment. Current RPLC SPP stationary phases applied  
205 for the separation of proteins and peptides are silica based, hydrophobically modified particles.  
206 For the analysis of moderate size proteins (15 - 20 kDa) and peptides, 1.3 - 3.6  $\mu\text{m}$  ( $\rho = 0.60$   
207 - 0.76), 100 - 200 Å pores size SPPs can be used with mechanical and thermal stability of 600  
208 - 1000 bar and 45 - 90°C, respectively. For the separation of larger proteins up to ~400 - 500  
209 kDa, 2.7 - 5.0  $\mu\text{m}$  ( $\rho = 0.63 - 0.90$ ), 200 - 1000 Å pores size SPPs are available and can be  
210 operated at 400 - 1000 bar and 60 - 90 °C. All of these materials are well suited for use in  
211 acidic and neutral conditions, and some of them can also withstand slightly basic mobile  
212 phases as well. Where no stability data is available, columns are suggested to be operated in  
213 conditions commonly used for similar particles (e.g. max. ~600 bar for 2.6 - 3.5  $\mu\text{m}$  particles,  
214 pH 2 - 7 and the lowest possible temperature at which adsorption can be avoided). Most of  
215 these widepore SPPs are modified with C18, C8 or C4 chains, some are C3, or phenyl modified  
216 using various bonding technologies. An exhaustive list of the RPLC SPPs commercially  
217 available for peptides and proteins applications are shown in Table 1.

218

### 219 **4. Current applications of wide-pore SPPs**

220 4.1. SPPs for the analysis of intact proteins and subunits

221 When separating proteins and peptides, several additional features have to be considered,  
222 compared to what is typically encountered with small molecules. One of the most important  
223 differences is the need for larger pores, to have full access to the surface and unrestricted  
224 intra-pore diffusion for large solutes. Thus, peptide separations generally require 100 - 200 Å  
225 pores, while 300 - 1000 Å pores are suitable for larger protein fragments and intact proteins.  
226 The second generation of widepore core-shell particles (Poroshell 300) showed excellent  
227 performance in bio-macromolecule separations [13]. Roth *et al.* packed these particles into 75  
228 µm x 150 mm capillaries and applied state-of-the-art MS analysis enabling the determination  
229 of intact proteins from complex matrices at sub-femtomole levels with excellent peak shapes  
230 and loading capacity [36]. The same material has been used for the separation of human IgG2  
231 disulfide isomers. The method has been qualified and allowed a fast separation of the isoforms,  
232 substantially improving the throughput [37]. Li *et al.* used a Poroshell 300 column for IgG  
233 biosimilarity studies [38]. Staub *et al.* compared the possibilities of 2.6 - 2.7 µm SSPs and 1.7  
234 µm fully porous materials using model peptides, tryptic digest and moderate size model  
235 proteins. In their work, 120 Å Poroshell and 100 Å Kinetex particles showed very similar  
236 performance to the 1.7 µm fully porous phase when separating ~12 - 64 kDa model proteins  
237 and peptides [39].

238 Variants of recombinant human Interferon alpha-2a have been analyzed using an Aeris  
239 Widepore C18 column. The method has been qualified and enabled the separation of the N-  
240 methionylated and oxidized variants in slightly degraded samples, more efficiently compared  
241 to the European Pharmacopeia RPLC method [40]. Separation performance of the same Aeris  
242 material was systematically evaluated in other studies and found to outperform various  
243 reference stationary phases when separating G-CSF oxidized and reduced variants [20], mAbs  
244 and mAb fragments [35,41]. Aeris Widepore columns have also been used for the separation  
245 of ADCs [27,42] and interferon related proteins [21]. It was demonstrated that depending on  
246 the gradient conditions (i.e. column length, gradient span and temperature), Aeris Widepore  
247 SPPs are suitable for both ultra-fast and ultra-high resolution separations of therapeutic  
248 proteins [41,43]. Loading capacity and kinetic efficiency of the latter was comparable to fully  
249 porous 1.7 µm particles. Interestingly, retention mechanism seemed to consist of a mixture of  
250 weak hydrophobic and pronounced strong polar interactions [21].

251 Morphology of wide pore SPP materials has been systematically optimized for intact protein  
252 and IgG subunit separations. It was found that 400 Å, 3.4 µm particles with 0.2 µm shell  
253 thickness and 1000 Å, 2.7 µm particles with 0.35 µm porous shell provided superior  
254 chromatographic performance for the separation of proteins up to ~ 400 kDa [24]. SPP  
255 particles of 1000 Å and 2.7 µm with 0.35 µm porous shell have been developed for the analysis  
256 of large proteins up to ~ 500 kDa and its efficiency has been compared to existing SPP and  
257 fully porous materials using a model mAb and various other model proteins [26]. Halo Protein

258 columns (3.4  $\mu\text{m}$  particles with 0.20  $\mu\text{m}$  shell thickness and 400  $\text{\AA}$ ) have been used for the  
259 analysis of IgGs and their fragments [27,44] and for the analysis of antibody drug conjugates  
260 [27,42].

261 Possibilities of new 3.5  $\mu\text{m}$  particles possessing 0.25  $\mu\text{m}$  shell and 450  $\text{\AA}$  pores (AdvanceBio  
262 RP-mAb) have been demonstrated by analyzing various model proteins, intact mAbs, their  
263 fragments and peptides [25,27,45], as well as ADCs [46,47].

264 Recently, a high coverage phenyl bonded SPP has been introduced under the name  
265 BioResolve RP-mAb. The material has been characterized and compared to reference  
266 widepore RPLC phases using intact and fragmented IgGs and ADC. It was found that this  
267 column advantageously marries the kinetic properties of modern SPPs with desirable chemical  
268 properties of some polymeric material (such as the Agilent PRLP-1 column) [27,48]. Figure 2  
269 shows some optimized separations of mAb and ADC subunits on a few selected columns  
270 packed with SPPs [27].

271

#### 272 4.2. SPPs for the analysis of peptides

273 SPPs with 160  $\text{\AA}$  pores (Halo Peptide) have been successfully applied for the analysis of  
274 peptides and moderate size proteins up to 15 kDa [17-19,49]. Staub *et al.* reported similar  
275 results for 2.6  $\mu\text{m}$  Kinetex and 2.7  $\mu\text{m}$  Poroshell 120 particles when separating model and  
276 tryptic peptides and comparing the separation power of these shell particles to 1.7  $\mu\text{m}$  fully  
277 porous ones [39]. Li *et al.* applied AdvanceBio (Poroshell 120) column for peptide mapping in  
278 biosimilarity studies [38].

279 Columns containing 2.6  $\mu\text{m}$  Kinetex particles were coupled into series to explore the  
280 possibilities of high resolution peptide mapping in 1D LC. The best kinetic performance was  
281 observed when coupling six columns of 150 mm, and operating the system at 1200 bar,  
282 yielding a flow rate close to the optimum of the van Deemter curve and resulting in peak  
283 capacity of 1360 for a 480 min gradient [50]. Kinetex 2.6  $\mu\text{m}$  column was used for the analysis  
284 of polypeptide antibiotics from food matrices [51]. Very fine prototype core-shell particles of 1.0  
285 - 1.4  $\mu\text{m}$  were also produced and tested using various analytes including tryptic digest. The  
286 finally commercialized 1.3  $\mu\text{m}$  SPPs showed 20 – 40 % higher peak capacities compared to  
287 the reference 1.7  $\mu\text{m}$  fully porous particles [52]. On the other hand, UHPLC systems with very  
288 low extra-column variance ( $< 10 \mu\text{l}^2$ ) and high operating pressures (e.g. 1200 - 1500 bar) must  
289 be used with such columns packed with 1.3  $\mu\text{m}$  SPP to attain their full benefits [53]. Tryptic  
290 mAb peptides were successfully separated on columns containing small core-shell particles of  
291 1.3, 1.6 and 1.7  $\mu\text{m}$ . The 1.3  $\mu\text{m}$  particles provided the best separation, but suffered from low  
292 permeability. Alternatively, 1.6 or 1.7  $\mu\text{m}$  shell particles can be applied since they showed  
293 comparable peak capacity at only two third of the operating pressure of 1.3  $\mu\text{m}$  particles [54].  
294 Indeed, 1.7  $\mu\text{m}$  SPPs showed ~50% improvement in plate heights compared to 1.7  $\mu\text{m}$  fully

295 porous materials when separating peptides and moderate size proteins, offering the possibility  
296 to achieve faster separations [16]. Figure 3 shows the separation of panitumumab tryptic  
297 peptides mAbs obtained on 1.3, 1.6 and 1.7  $\mu\text{m}$  SPPs using the same chromatographic  
298 conditions [54]. Interestingly, due to differences in diffusion properties, 1.3  $\mu\text{m}$  particles  
299 seemed to be more favourable for the separation of peptides than for small molecules when  
300 using longer columns and longer gradient times [55]. Finally, the 1.6  $\mu\text{m}$  SPPs have been used  
301 for the determination of PEGprotein from biological matrix following tryptic digestion [56].

302 For interested readers, numerous further applications can be found in brochures of  
303 manufacturers reflecting that widepore SPP technology has gained more and more interest in  
304 modern analytical laboratories. Stability of wide pore SPPs at high temperatures and acidic  
305 conditions, generally applied in peptides and proteins separations are also demonstrated in  
306 many of those documents.

307

### 308 **5. Current trends and possible developments in SPP technology**

309 The thickness of the porous shell of SPPs influences both the separation power and retention.  
310 Decreasing the thickness of the porous layer potentially results in lower values of the  $C$ -term  
311 and minimum plate heights [57]. Poppe plots calculated for various shell thickness predict that  
312 the analysis time to attain a given peak capacity decreases significantly with decreasing  
313 thickness of the porous layer, but this gain is more important for large molecules [57]. However  
314 the eluent strength has to be reduced to compensate for the decrease in retention caused by  
315 the reduction of the stationary phase surface area (decrease of volume fraction). Figure 4  
316 shows the impact of shell thickness on the plate height ( $h$ ) as a function of mobile phase  
317 velocity ( $v$ ) for peptides and proteins.

318 An interesting idea was suggested by Guiochon and co-workers to increase efficiency with  
319 SPPs for large molecules [58]. Mass transfer kinetics of proteins was found to be the fastest  
320 for columns packed with SPP particles having either a large core-to-particle ratio or having a  
321 second, external shell (bi-shell particle) made of a thin porous layer with large mesopores (200  
322 – 300  $\text{\AA}$ ) and high porosity (50 – 70 %). The structure of this external shell seems to speed up  
323 the penetration of proteins into the particles.

324 All the above mentioned fundamental studies suggest that thinner shells and larger pore  
325 diameters can further improve the efficiency of current SPPs for large molecule separations.  
326 As today, mAbs and related compounds ( $\text{MW} \geq 150 \text{ kDa}$ ) seem to be the most promising  
327 candidates of protein therapeutics, the common wide-pore SPPs (possessing 200 – 300  $\text{\AA}$   
328 pore diameter) need to be revised. To further optimize the efficiency of commercially available  
329 wide-pore SPPs, recently 400, 450 and 1000  $\text{\AA}$  SPPs were commercialized to analyse large  
330 proteins in reversed phase (RP) chromatography [24,25,26,27].

331 Today, SPPs are mostly used for RP of proteins however obviously, SPP advantages exist in  
332 most modes of liquid chromatography (sorptive modes) and therefore new SPPs are expected  
333 in hydrophobic interaction chromatography (HIC), hydrophilic interaction liquid  
334 chromatography (HILIC) and ion-exchange (IEX), as these modes are routinely used for  
335 protein characterization. Recently a HILIC 2.6  $\mu\text{m}$  SPP was introduced for released and  
336 labelled glycan analysis of proteins [59]. This column contains a unique titanium based  
337 biocompatible hardware and frits.

338 Surprisingly, it seems that SPPs can provide high efficiency in size exclusion chromatography  
339 (SEC) as well. The thermodynamic retention factor and therefore the useful elution window is  
340 indeed limited by the ratio of pore porosity (internal) and external porosity in SEC. Therefore,  
341 large pore volume is thermodynamically advantageous in SEC, and this is why porous particles  
342 provide wider elution window and more chance to separate compounds (improved selectivity).  
343 Despite this expected behaviour, a few recent publications showed that the loss of pore volume  
344 of SPPs can be compensated by the shortening of the solute diffusion length inside the pores  
345 [26,60,61]. Then, even if the elution window is narrower, similar efficiency can be achieved due  
346 to the narrower peaks. Moreover, the analysis time can be shortened in proportion to the  
347 internal porosity.

348

#### 349 5.1. Radially oriented mesopores (ROM-SPP)

350 Very recently, the so-called radially oriented mesoporous SPPs were proposed to decrease  
351 longitudinal diffusion and hence to improve the overall separation efficiency. A new process  
352 was developed (called as pseudomorphic transformation (PMT)), which is a form of micelle  
353 templating. This PMT technology produces straight, unconnected, and radially-oriented  
354 mesopores (ROMs) (Figure 5.). SPP particles with ROMs possess many advantages such as  
355 a narrower particle size distribution, thinner porous layer with high surface area and - most  
356 importantly - highly ordered, non-tortuous pore channels oriented perpendicular to the particle  
357 surface [62]. The improved efficiency of such ROMs mostly related to a smaller *B*-term  
358 probably due to the thinner porous layer and/or the unique, ordered porous straight channels.  
359 In addition, Poppe plot calculations showed superior performance of these PMT-SPPs across  
360 the entire analysis time range compared to conventional SPPs and fully porous particles. A  
361 theoretical study also confirmed the gain in longitudinal diffusion, but this gain is only  
362 interesting for molecules possessing high diffusivity (small molecules) [63].

363 Gritti assumed various pore shapes for ROMs in a fundamental study [64]. It was found that  
364 the eddy dispersion does not depend on neither the pore structure nor the shape. However,  
365 when assuming conical mesopore shape a decrease in *C*-term is expected. Therefore, this  
366 conical shape ROM material suits well for protein separations.

367 In agreement with the theory, some ROM SPPs have already been recently applied for large  
368 molecule separations. The pore size of silica SPPs with fibrous shell structure could be tuned  
369 by using organic solvents of different polarities [65]. By using benzene as oil phase, SPPs with  
370 pore size of up to 370 Å and surface area of 61 m<sup>2</sup>/g were prepared and successfully applied  
371 for the rapid separation of small solutes, peptides, and proteins. The wide pores of the porous  
372 spheres were especially useful for separating large proteins with excellent efficiency without  
373 restricted diffusion [65].

374

## 375 5.2. Molecularly imprinted polymers

376 Molecularly imprinted polymers (MIPs) have been utilized as recognition elements for a wide  
377 range of analytes due to their high stability and remarkable mechanical properties. However,  
378 the traditional MIPs suffered from some limitations for practical applications. To broaden the  
379 application scope, multifunctional SPP MIPs have attracted increasing attention in separation.  
380 A current review discusses the recent developments of MIPs with a nonimprinted core  
381 (Core@MIP particles) and MIPs with a non-imprinted shell (MIP@Shell particles) [66]. In  
382 addition, other novel miscellaneous SPP MIPs with a hollow-core, a semi-shell, or an empty-  
383 shell are summarized.

384

## 385 5.3. Magnetic materials

386 The separation and enrichment of proteins and peptides from complex mixtures is of great  
387 importance to provide a successful identification. Core–shell structured magnetic  
388 microspheres have been widely used for the enrichment and isolation of proteins and peptides,  
389 thanks to their unique properties such as strong magnetic responsiveness, outstanding binding  
390 capacity, excellent biocompatibility, robust mechanical strength and admirable recovery [67].  
391 The advances in the application of core–shell structured magnetic materials for proteomic  
392 analysis, including the separation and enrichment of low-concentration proteins and peptides,  
393 the selective enrichment of phosphoproteins and the selective enrichment of glycoproteins  
394 were recently reviewed by Deng *et al.* [67]. Although much progress has been made in the  
395 application of core–shell structured magnetic microspheres to the enrichment of low-  
396 abundance peptides, the design of novel functionalized magnetic nanocomposites with well-  
397 defined nanostructures and surface properties for the application in proteomics remains an  
398 area of intense research interest.

399

## 400 5.4. Chiral separations

401 In the field of enantioseparations by LC, we can expect a real revolution thanks to the use of  
402 chiral SPPs of latest generation [68]. Over the years, this field has fallen behind compared to  
403 achiral RP separations as regards ultrafast and highly efficient separations. However, new

404 developments in chiral particle technology may change this trend. In particular, extraordinary  
405 results and very fast enantioseparations are expected by the employment of latest generation  
406 chiral particles in supercritical fluid chromatography (SFC) [69]. Moreover, chiral stationary  
407 phases made on SPPs could be suitable, thanks to their high efficiency, in the case of  
408 challenging enantiomeric separations (e.g., chiral impurity profiling), where an extremely low  
409 concentration of one enantiomer has to be detected [70].

410

## 411 **6. Conclusion**

412 Columns packed with superficially porous particles are widely used in LC and gain more and  
413 more interest over the years thanks to their excellent kinetic performance and moderate  
414 operating pressure. Standard pore materials (90 – 120 Å) became very successful in the last  
415 decade for small molecule separations. Thanks to new developments, widepore SPPs are now  
416 also available and offer new possibilities for large molecule separations.

417 As the pore diameter is larger and shells are thinner, the mass transfer kinetics becomes faster  
418 for large solutes (possessing low diffusivity). For such reasons, very efficient separations are  
419 routinely achieved on these materials. Current particle structures and pore sizes applied for  
420 peptides (100 – 200 Å) and proteins (200 – 1000 Å) separations with very thin porous layer  
421 seem to be close to the optimal morphology. Various chemistries are being developed to avoid  
422 undesired secondary interactions which often lead to significant band broadening and poor  
423 recovery.

424 Second and third generation SPPs are now regularly used for the analysis of therapeutic  
425 proteins, mAbs, ADCs and related proteins at intact, sub-unit and peptide levels. Very high  
426 peak capacity can be attained on 50 – 150 mm long columns, typically within 5 – 15 minutes.  
427 When combining the exceptional kinetic performance of wide pore SPPs with the reliability of  
428 computer assisted retention modeling, significant resources can be saved during method  
429 development. From initial experiments to robustness testing and documentation of the  
430 optimized method, the whole process usually takes only few working days.

431 Future trends in SPP developments are focused on further morphology optimizations and  
432 finding new fields of application. Radially oriented mesopores with various shapes show  
433 significant advantages in diffusion properties which can be beneficial for the separation of large  
434 molecules.

435

## 436 **Acknowledgements**

437 Davy Guillarme wishes to thank the Swiss National Science Foundation for support through a  
438 fellowship to Szabolcs Fekete (31003A 159494).

439

440 **References**

- 441 [1] S. Fekete, E. Olah, J. Fekete, Fast liquid chromatography: The domination of core-shell  
442 and very fine particles, *J. Chromatogr. A* 1228 (2012) 57-71.
- 443 [2] G. Guiochon, F. Gritti, Shell particles, trials, tribulations and triumphs, *J. Chromatogr. A*  
444 1218 (2011) 1945-1938.
- 445 [3] J.H. Knox, Evidence for turbulence and coupling in chromatographic columns, *Anal. Chem.*  
446 38 (1966) 253-261.
- 447 [4] C. Horvath, B.A. Preiss, S.R. Lipsky, Fast liquid chromatography. Investigation of operating  
448 parameters and the separation of nucleotides on pellicular ion exchangers, *Anal. Chem.* 39  
449 (1967) 1422-1428.
- 450 [5] C. Horvath, S.R. Lipsky, Column design in high pressure liquid chromatography *J.*  
451 *Chromatogr. Sci.* 7 (1969) 109-116.
- 452 [6] J.J. Kirkland, Controlled surface porosity supports for high-speed gas and liquid  
453 chromatography, *Anal. Chem.* 41 (1969) 218-220.
- 454 [7] J.J. Kirkland, Superficially porous silica microspheres for the fast high-performance liquid  
455 chromatography of macromolecules, *Anal. Chem.* 64 (1992) 1239-1245.
- 456 [8] J.N. Done, J.H. Knox, The performance of packings in high speed liquid chromatography  
457 II. ZIPAX® the effect of particle size *J. Chromatogr. Sci.* 10 (1972) 606-615.
- 458 [9] T. Issaeva, A. Kourganov, K. Unger, Super-high-speed liquid chromatography of proteins  
459 and peptides on non-porous Micra NPS-RP packings, *J. Chromatogr. A* 846 (1999) 13-23.
- 460 [10] T.J. Barder, P.J. Wohlman, C. Thrall, P.D. DuBois, Fast chromatography and non-porous  
461 silica, *LC–GC* 15 (1997) 918-926.
- 462 [11] R.M. Seifar, J.C. Kraak, W.Th. Kok, H. Poppe, Capillary electrochromatography with 1.8-  
463  $\mu\text{m}$  ODS-modified porous silica particles, *J. Chromatogr. A* 808 (1998) 71-77.
- 464 [12] N. Wu, Y. Liu, M.L. Lee, Sub-2 microm porous and nonporous particles for fast separation  
465 in reversed-phase high performance liquid chromatography, *J. Chromatogr. A* 1131 (2006)  
466 142-150.
- 467 [13] J.J. Kirkland, F.A. Truszkowski, C.H. Dilks Jr., G.S. Engel, Superficially porous silica  
468 microspheres for fast high-performance liquid chromatography of macromolecules, *J.*  
469 *Chromatogr. A* 890 (2000) 3–13.
- 470 [14] S. Fekete, J. Fekete, K. Ganzler, Shell and small particles; Evaluation of new column  
471 technology, *J. Pharm. Biomed. Anal.* 49 (2009) 64-71.
- 472 [15] E. Olah, S. Fekete, J. Fekete, K. Ganzler, Comparative study of new shell-type, sub-2  $\mu\text{m}$   
473 fully porous and monolith stationary phases, focusing on mass-transfer resistance, *J.*  
474 *Chromatogr. A*, 1217 (2010) 3642-3653.

475 [16] S. Fekete, K. Ganzler, J. Fekete, Efficiency of the new sub-2  $\mu\text{m}$  core–shell (Kinetex™)  
476 column in practice, applied for small and large molecule separation, *J. Pharm. Biomed. Anal.*  
477 54 (2011) 482–490.

478 [17] F. Gritti, G. Guiochon, The mass transfer kinetics in columns packed with Halo-ES shell  
479 particles, *J. Chromatogr. A* 1218 (2011) 907–921.

480 [18] S.A. Schuster, B.M. Wagner, B.E. Boyes, J.J. Kirkland, Wider pore superficially porous  
481 particles for peptide separations by HPLC, *J. Chromatogr. Sci.* 48 (2010) 566–571.

482 [19] S.A. Schuster, B.E. Boyes, B.M. Wagner, J.J. Kirkland, Fast high performance liquid  
483 chromatography separations for proteomic applications using Fused-Core® silica particles, *J.*  
484 *Chromatogr. A* 1228 (2012) 232–241.

485 [20] S. Fekete, R. Berky, J. Fekete, J.L. Veuthey, D. Guillarme, Evaluation of a new wide pore  
486 core–shell material (Aeris™ WIDEPORÉ) and comparison with other existing stationary  
487 phases for the analysis of intact proteins, *J. Chromatogr. A* 1236 (2012) 177–188.

488 [21] S. Fekete, R. Berky, J. Fekete, J.L. Veuthey, D. Guillarme, Evaluation of recent very  
489 efficient wide-pore stationary phases for the reversed-phase separation of proteins, *J.*  
490 *Chromatogr. A* 1252 (2012) 90–103.

491 [22] S. Fekete, J.L. Veuthey, D.V. McCalley, D. Guillarme, The effect of pressure and mobile  
492 phase velocity on the retention properties of small analytes and large biomolecules in ultrahigh  
493 pressure liquid chromatography, *J. Chromatogr. A*, 1270 (2012) 127–138.

494 [23] S. Fekete, D. Guillarme, Estimation of pressure-, temperature- and frictional heating-  
495 related effects on proteins' retention under ultra-high-pressure liquid chromatographic  
496 conditions, *J. Chromatogr. A*, 1393 (2015) 73–80.

497 [24] S.A. Schuster, B.M. Wagner, B.E. Boyes, J.J. Kirkland, Optimized superficially porous  
498 particles for protein separations, *J. Chromatogr. A* 1315 (2013) 118–126.

499 [25] W. Chen, K. Jiang, A. Mack, B. Sachok, X. Zhu, W.E. Barber, X. Wang, Synthesis and  
500 optimization of wide pore superficially porous particles by a one-step coating process for  
501 separation of proteins and monoclonal antibodies, *J. Chromatogr. A* 1414 (2015) 147–157.

502 [26] B.M. Wagner, S.A. Schuster, B.E. Boyes, T.J. Shields, W.L. Miles, M.J. Haynes, R.E.  
503 Moran, J.J. Kirkland, M.R. Schure, Superficially porous particles with 1000 Å pores for large  
504 biomolecule high performance liquid chromatography and polymer size exclusion  
505 chromatography, *J. Chromatogr. A* 1489 (2017) 75–85.

506 [27] B. Bobaly, M. Lauber, A. Beck, D. Guillarme, S. Fekete, Utility of a high coverage phenyl-  
507 bonding and wide-pore superficially porous particle for the analysis of monoclonal antibodies  
508 and related products, *J. Chromatogr. A*, 1549 (2018) 63–76.

509 [28] J.J. van Deemter, F.J. Zuiderweg, A. Klinkenberg, Longitudinal diffusion and resistance to  
510 mass transfer as causes of nonideality in chromatography, *Chem. Eng. Sci.* 5 (1956) 271–289.

511 [29] P.A. Bristow, J.H. Knox, Standardization of test conditions for high performance liquid  
512 chromatography columns, *Chromatographia*, 6 (1977) 279-289.

513 [30] S. Deridder, G. Desmet, Effective medium theory expressions for the effective diffusion in  
514 chromatographic beds filled with porous, non-porous and porous-shell particles and cylinders.  
515 Part II: Numerical verification and quantitative effect of solid core on expected B-term band  
516 broadening, *J. Chromatogr. A*, 1218 (2011) 46-56.

517 [31] D. Cabooter, A. Fanigliulo, G. Bellazzi, B. Allieri, A. Rottigni, G. Desmet, Relationship  
518 between the particle size distribution of commercial fully porous and superficially porous high-  
519 performance liquid chromatography column packings and their chromatographic performance,  
520 *J. Chromatogr. A*, 1217 (2010) 7074-7081.

521 [32] F. Gritti, I. Leonardis, J. Abia, G. Guiochon, Physical properties and structure of fine core-  
522 shell particles used as packing materials for chromatography: Relationships between particle  
523 characteristics and column performance, *J. Chromatogr. A*, 1217 (2010) 3819-3843.

524 [33] S. Fekete, D. Guillarme, M. Dong, Superficially porous particles: Perspectives, practices  
525 and trends, *LCGC North Am.*, 32 (2014) 420-433.

526 [34]. V. Gonzalez-Ruiz, A. I. Olives, M. A. Martin, Core-shell particles lead the way to renewing  
527 high-performance liquid chromatography, *Trends Anal. Chem.* 64 (2015) 17-28.

528 [35]. S. Fekete, J.-L. Veuthey, D. Guillarme, Achievable separation performance and analysis  
529 time in current liquid chromatographic practice for monoclonal antibody separations, *J. Pharm.*  
530 *Biomed. Anal.* 141 (2017) 59-69.

531 [36]. M. J. Roth, D. A. Plymire, A. N. Chang, J. Kim, E. M. Maresh, S. E. Larson, S. M. Patrie,  
532 Sensitive and Reproducible Intact Mass Analysis of Complex Protein Mixtures with  
533 Superficially Porous Capillary Reversed-Phase Liquid Chromatography Mass Spectrometry,  
534 *Anal. Chem.* 83 (2011) 9586-9592.

535 [37]. Q. Wang, N. A. Lacher, B. K. Muralidhara, M. R. Schlittler, S. Aykent, C. W. Demarest,  
536 Rapid and refined separation of human IgG2 disulfide isomers using superficially porous  
537 particles, *J. Sep. Sci.* 33 (2010) 2671-2680.

538 [38]. W. Li, B. Yang, D. Zhou, J. Xu, Z. Ke, W.-C. Suen, Discovery and characterization of  
539 antibody variants using massspectrometry-based comparative analysis for biosimilar  
540 candidates of monoclonal antibody drugs, *J. of Chromatogr. B*, 1025 (2016) 57-67.

541 [39]. A. Staub, D. Zurlino, S. Rudaz, J.-L. Veuthey, D. Guillarme, Analysis of peptides and  
542 proteins using sub-2  $\mu\text{m}$  fully porous and sub 3- $\mu\text{m}$  shell particles, *J. Chromatogr. A*, 1218  
543 (2011) 8903-8914.

544 [40]. Y. Lia, C. Rao, L. Tao, J. Wang, B. Lorbetkie, M. Girard, Improved detection of variants  
545 in recombinant human interferon alpha-2a products by reverse-phase high-performance liquid  
546 chromatography on a core-shell stationary phase, *J. Pharm. Biomed. Anal.* 88 (2014) 123-  
547 129.

548 [41]. S. Fekete, D. Guillarme, Reversed-phase liquid chromatography for the analysis of  
549 therapeutic proteins and recombinant monoclonal antibodies, *LCGC Europe*, 25 (2012) 540-  
550 550.

551 [42]. S. Fekete, M. Rodriguez-Aller, A. Cusumano, R. Hayes, H. Zhang, T. Edge, J.-L. Veuthey,  
552 D. Guillarme, Prototype sphere-on-sphere silica particles for the separation of large  
553 biomolecules, *J. Chromatogr. A*, 1431 (2016) 94-102.

554 [43]. S. Fekete, M. W. Dong, T. Zhang, D. Guillarme, High resolution reversed phase analysis  
555 of recombinant monoclonal antibodies by ultra-high pressure liquid chromatography column  
556 coupling, *J. Pharm. Biomed. Anal.* 83 (2013) 273-278.

557 [44]. B. Wei, B. Zhang, B. Boyes, Y. T. Zhang, Reversed-phase chromatography with large  
558 pore superficially porous particles for high throughput immunoglobulin G2 disulfide isoform  
559 separation, *J. Chromatogr. A*, 1526 (2017) 104-111.

560 [45]. K. Sandra, M. Steenbeke, I. Vandenhede, G. Vanhoenacker, P. Sandra, The versatility  
561 of heart-cutting and comprehensive two-dimensional liquid chromatography in monoclonal  
562 antibody clone selection, *J. Chromatogr. A*, 1523 (2017) 283-292.

563 [46]. S. Fekete, I. Molnár, D. Guillarme, Separation of antibody drug conjugate species by  
564 RPLC: A generic method development approach, *J. Pharm. Biomed. Anal.* 137 (2017) 60-69.

565 [47]. K. Sandra, G. Vanhoenacker, I. Vandenhede, M. Steenbeke, M. Joseph, P. Sandra,  
566 Multiple heart-cutting and comprehensive two-dimensional liquid chromatography hyphenated  
567 to mass spectrometry for the characterization of the antibody-drug conjugate ado-trastuzumab  
568 emtansine, *J. Chromatog. B*, 1032 (2016) 119-130.

569 [48]. B. Bobály, V. D'Atri, M. Lauber, A. Beck, D. Guillarme, S. Fekete, Characterizing various  
570 monoclonal antibodies with milder reversed phase chromatography conditions, *J. Chromatogr.*  
571 *B*, submitted

572 [49]. J. J. Kirkland, S. A. Schuster, W. L. Johnson, B. E. Boyes, Fused-core particle technology  
573 in high-performance liquid chromatography: An overview, *J. Pharm. Anal.* 3 (2013) 303-312.

574 [50]. J. De Vos, C. Stassen, A. Vaast, G. Desmet, S. Eeltink, High-resolution separations of  
575 tryptic digest mixtures using core-shell particulate columns operated at 1200 bar, *J.*  
576 *Chromatogr. A*, 1264 (2012) 57-62.

577 [51]. A. Kaufmann, M. Widmer, Quantitative analysis of polypeptide antibiotic residues in a  
578 variety of food matrices by liquid chromatography coupled to tandem mass spectrometry, *Anal.*  
579 *Chim. Acta*, 797 (2013) 81-88.

580 [52]. A. C. Sanchez, G. Friedlander, S. Fekete, J. Anspach, D. Guillarme, M. Chitty, T. Farkas,  
581 Pushing the performance limits of reversed-phase ultra-high performance liquid  
582 chromatography with 1.3  $\mu\text{m}$  core-shell particles, *J. Chromatogr. A*, 1311 (2013) 90-97.

583 [53]. S. Fekete, D. Guillarme, Kinetic evaluation of new generation of column packed with  
584 1.3  $\mu\text{m}$  core-shell particles, *J. Chromatogr. A*, 1308 (2013) 104-113.

585 [54]. B. Bobaly, D. Guillarme, S. Fekete, Systematic comparison of a new generation of  
586 columns packed with sub-2  $\mu\text{m}$  superficially porous particles, *J. Sep. Sci.* 37 (2014) 189-197.

587 [55] S. Fekete, D. Guillarme, Possibilities of new generation columns packed with 1.3  $\mu\text{m}$  core-  
588 shell particles in gradient elution mode, *J. Chromatogr. A*, 1320 (2013) 86-95.

589 [56]. N. Zheng, J. Zeng, A. Manney, L. Williams, A.-F. Aubry, K. Voronin, A. Buzescu, Y. J.  
590 Zhang, A. Allentoff, C. Xu, H. Shen, W. Warner, M. E. Arnold, Quantitation of a PEGylated  
591 protein in monkey serum by UHPLC-HRMS using a surrogate disulfide-containing peptide: A  
592 new approach to bioanalysis and in vivo stability evaluation of disulfide-rich protein  
593 therapeutics, *Anal. Chim. Acta*, 916 (2016) 42-51.

594 [57] K. Horvath, F. Gritti, J.N. Fairchild, G. Guiochon, On the optimization of the shell thickness  
595 of superficially porous particles, *J. Chromatogr. A*, 1217 (2010) 6373-6381.

596 [58] F. Gritti, K. Horvath, G. Guiochon, How changing the particle structure can speed up  
597 protein mass transfer kinetics in liquid chromatography, *J. Chromatogr. A*, 1263 (2012) 84-98.

598 [59] <http://www.phenomenex.com/products/detail/biozen> accessed: 15.04.2018

599 [60] M.R. Shure, R.E. Moran, Size exclusion chromatography with superficially porous  
600 particles, *J. Chromatogr. A* 1480 (2017) 11-19.

601 [61] B.W.J. Pirok, P. Breuer, S. J.M. Hoppe, M. Chitty, E. Welch, T. Farkas, S. van der Wal, R.  
602 Peters, P.J. Schoenmakers, Size-exclusion chromatography using core-shell particles, *J.*  
603 *Chromatogr. A* 1486 (2017) 96-102.

604 [62] T.C. Wei, A. Mack, W. Chen, J. Liu, M. Dittmann, X. Wang, W.E. Barber, Synthesis,  
605 characterization, and evaluation of a superficially porous particle with unique, elongated pore  
606 channels normal to the surface, *J. Chromatogr. A* 1440 (2016) 55-65.

607 [63] S. Deridder, M. Catani, A. Cavazzini, G. Desmet, A theoretical study on the advantage of  
608 core-shell particles with radially-oriented mesopores, *J. Chromatogr. A* 1456 (2016) 137-144.

609 [64] F. Gritti, Impact of straight, unconnected, radially-oriented, and tapered mesopores on  
610 column efficiency: a theoretical investigation, *J. Chromatogr. A* 1485 (2017) 70-81.

611 [65] Q. Qu, Y. Si, H. Xuan, K. Zhang, X. Chen, Y. Ding, S. Feng, H.Q. Yu, M. A. Abdullah, K.A.  
612 Alamry, Dendritic core-shell silica spheres with large pore size for separation of biomolecules,  
613 *J. Chromatogr. A* 1540 (2018) 31-37.

614 [66] L. Wan, Z. Chen, C. Huang, X. Shen, Core-shell molecularly imprinted particles, *TrACs*,  
615 95 (2017) 110-121.

616 [67] M. Zhao, Y. Xie, C. Deng, X. Zhang, Recent advances in the application of core-shell  
617 structured magnetic materials for the separation and enrichment of proteins and peptides, *J.*  
618 *Chromatogr. A* 1357 (2014) 182-193.

619 [68] M. Catani, S. Felletti, O.H. Ismail, F. Gasparrini, L. Pasti, N. Marchetti, C. De Luca, V.  
620 Costa, A. Cavazzini, New frontiers and cutting edge applications in ultrahigh performance

621 liquid chromatography through latest generation superficially porous particles with particular  
622 emphasis to the field of chiral separations, *Anal. Bioanal. Chem.*, 410 (2018) 2457-2465.  
623 [69] L. Sciascera, O.H. Ismail, A. Ciogli, D. Kotoni, A. Cavazzini, L. Botta, T. Szczerba, J.  
624 Kocergin, C. Villani, F. Gasparrini, Expanding the potential of chiral chromatography for high-  
625 throughput screening of large compound libraries by means of sub-2  $\mu\text{m}$  Whelk-O 1 stationary  
626 phase in supercritical fluid conditions, *J Chromatogr A*. 1383 (2015) 160–168.  
627 [70] G. Mazzocanti, O.H. Ismail, I. D'Acquarica, C. Vilani, C. Manzo, M. Wilcox, A. Cavazzini,  
628 F. Gasparrini, Cannabis through the looking glass: chemo- and enantio-selective separation  
629 of phytocannabinoids by enantioselective ultrahigh performance supercritical fluid  
630 chromatography, *Chem Commun*. 53 (2017) 12262–12265.  
631  
632

633 **9. Figure/Table captions**

634

635 Table 1. List and physico-chemical properties of currently available SPPs applied for peptides  
636 and proteins separations.

637

638 Figure 1. History of the development of SPP phases. The source of pictures/drawings (papers)  
639 used for this figure are referred during the text of this review. The particles (spheres) in colour  
640 are taken from available (free) brochures from different column providers.

641

642 Figure 2. Optimized separations of mAb (A) and ADC (B) subunits on selected columns packed  
643 with SPP. Illustration is based on a figure published in ref [27].

644

645 Figure 3. Chromatograms of a tryptic digest of Panitumumab on Cortecs 1.6  $\mu\text{m}$  (A), Kinetex  
646 1.7  $\mu\text{m}$  (B) and Kinetex 1.3  $\mu\text{m}$  (C). Mobile phase A: 0.1% TFA in water, B: 0.1% TFA in ACN.  
647 Flow rate: 0.5 mL/min, gradient: 10–30% B in 10 min. Column temperature 30  $^{\circ}\text{C}$ , detection:  
648 UV at 210 nm (with permission from ref [54]).

649

650 Figure 4. Structure of a SPP (A) and calculated plate height curves for model peptide (B) and  
651 model protein (C) assuming various SPP structure with  $\rho = 0, 0.5, 0.7, 0.85$  and 1 (with  
652 permission from ref [57]).

653

654 Figure 5. Schematic view of radially oriented SPP (A) and conventional SPP (B) (cross section  
655 view). Black arrows indicate the solute diffusion.

column name			particle size (µm)	core (µm)	rho	pore size (Å)	max Temperature (°C)	pH range	max pressure (bar)	total porosity	permeability (cm <sup>2</sup> ·10 <sup>-11</sup> )	
Aeris (Phenomenex)	Widepore	XB-C18	3.6	3.2	0.89	~ 200	90	1.5-9	600	0.52	21 [25]	
		XB-C8 <sup>§</sup>										
		C4 <sup>§</sup>										
	Peptide/Kinetex	XB-C18	1.7 <sup>§</sup>	1.3	0.76	100	90		1000	0.56	3.1 [40]	
			2.6 <sup>§</sup>	1.9	0.73				600	0.52	5.8 [39]	
			3.6	2.6	0.72				n.a.	n.a.		
Halo (Advanced Materials Technology)	Protein	ES-C18	3.4 <sup>#</sup>	3	0.88	400	90	1-8	600	0.58	26 [25]	
			2.7	2	0.74	1000				0.35	6.4 [39]	
		C4	3.4 <sup>#</sup>	3	0.88	400				2-9	0.58	26 [25]
			2.7 <sup>#</sup>	2	0.74	1000					0.35	6.4 [39]
	Peptide	ES-C18	2.0 <sup>#</sup>	1.2	0.6	160	90	1-8	1000	n.a.	n.a.	
			2.7 <sup>**</sup>	1.7	0.63				600	0.35	6.4 [39]	
			4.6 <sup>#</sup>	3.3	0.72				n.a.	n.a.		
		ES-CN	2.7 <sup>#</sup>	1.7	0.63				0.35	6.4 [39]		
			4.6 <sup>#</sup>	3.3	0.72				n.a.	n.a.		
			Pheny-Hexyl	2.7	1.7				0.63	2-9	0.35	6.4 [39]
	AdvanceBio (Agilent)	RP-mAb	C4	3.5	3	0.86	450	90	1-8	600	0.56	18 [25]
			SB-C8									
Diphenyl												
Peptide Mapping		EC-C18	2.7	1.7	0.63	120	60	2-8	600	0.37	4.6 [39]	
Peptide Plus	charged C18											
Accucore (Thermo)	150	C18	2.6	1.6	0.62	150	60	1-11	1000	n.a.	n.a.	
	150	C4						2-9				
Poroshell (Agilent)	300	SB-C18	5	4.5	0.9	300	90	1-8	400	0.62	73 [41]	
		SB-C8										
		SB-C3										
		Extend-C18										
BioResolve (Waters)	RP mAb	Polyphenyl	2.7	1.9	0.7	450	90	2-7	689	0.65	14 [25]	
Cortecs (Waters)		C18	1.6	1.1	0.7	90	45	2-8	1000	0.56	3.5 [40]	
			2.7	1.9	0.7					n.a.	n.a.	
Meteoric Core (YMC)	BIO	C18	2.7	1.7	0.7	160	70	1.5-10	600	n.a.	n.a.	
SpeedCore Bio (Fortis)	Peptide	C18	2.6	2	0.77	160	80	1-8	600	n.a.	n.a.	
			2.6	2	0.77	160				n.a.	n.a.	
	Protein	C18	3.5	3.1	0.89	300				n.a.	n.a.	
		C8								n.a.	n.a.	
Capcell (Shiseido) Core	MP	C18	2.7	1.7	0.63	160	n.a.	2-10	600	n.a.	n.a.	
	WP					300			480	n.a.	n.a.	
SunShell (Chromanik Technologies)	WP	C18	2.6	1.6	0.62	160	n.a.	1.5-10	600	n.a.	n.a.	
Aurashell (Horizon)	PEP	C18	2.7	1.7	0.63	200	n.a.	1-9	n.a.	n.a.	n.a.	
	PRO	C18	3.5	3	0.86	300	n.a.		n.a.	n.a.	n.a.	

\*these phases are available packed into biocompatible titanium infused flow path column hardware under the name of bioZen

\*this phase is available under the brand names of Ascentis (Supelco) Express Peptide ES-C18 and Brownlee (Perkin Elmer) SPP Peptide ES-C18

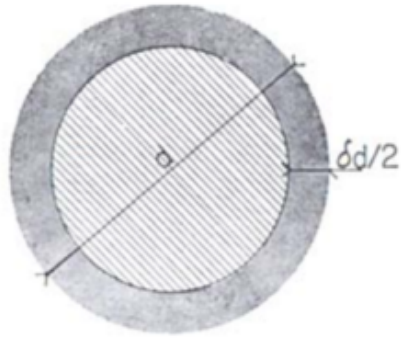
#these phases are available under the brand names of Bioshell (Supelco) A160 Peptide, A400 Protein and IgG 1000Å

Table 1

**Knox:**

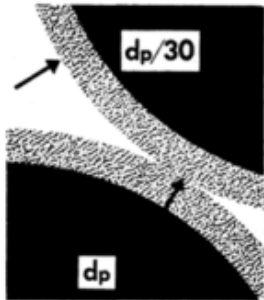
Idea of thin films for stationary phase

**Horvath and co-workers:**  
50 µm pellicular particles



**Kirkland:**

30-40 µm controlled surface porosity supports

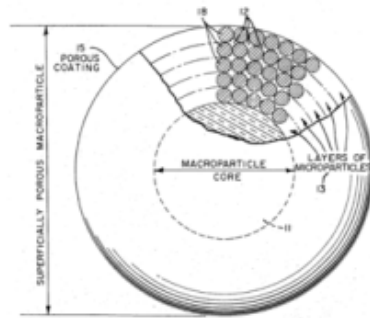


**Commercially available  
30-50 µm, 1st generation SPPs:**

Zipax® (DuPont)

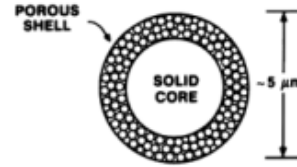
Corasil® (Waters Associates)

Pellicosil® (Macherey-Nagel)

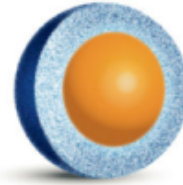


**5 µm and sub-3 µm 2nd generation SPPs:**

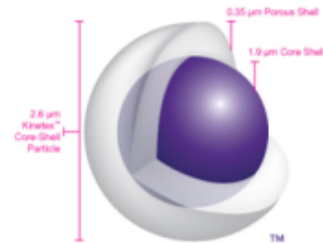
Poroshell® (Agilent)



Halo® (AMT)



Kinetex® (Phenomenex)



**Widepore SPPs:**

Halo® Protein and Peptide (AMT)



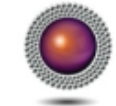
Aeris® (Phenomenex)



AdvanceBio® (Agilent)



Accucore® (Thermo)



BioResolve® (Waters)



**Sub-2 µm 3rd generation SPPs:**

Kinetex® (Phenomenex)



Cortecs® (Waters)



**Market diversification for sub-3 µm SPPs**

1960s

1970-1990s

2000s

2010s

Figure 1

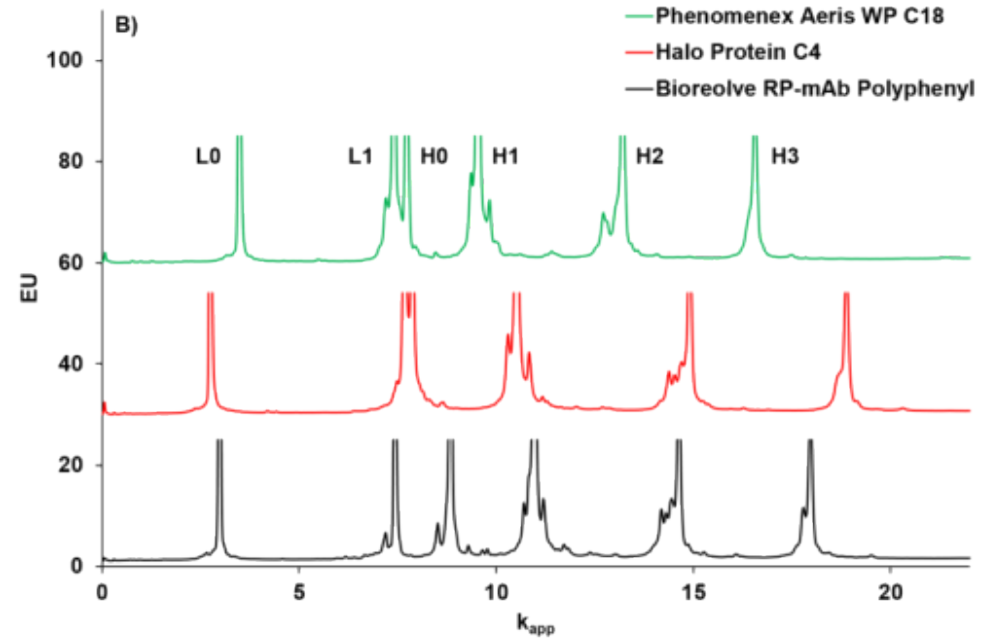
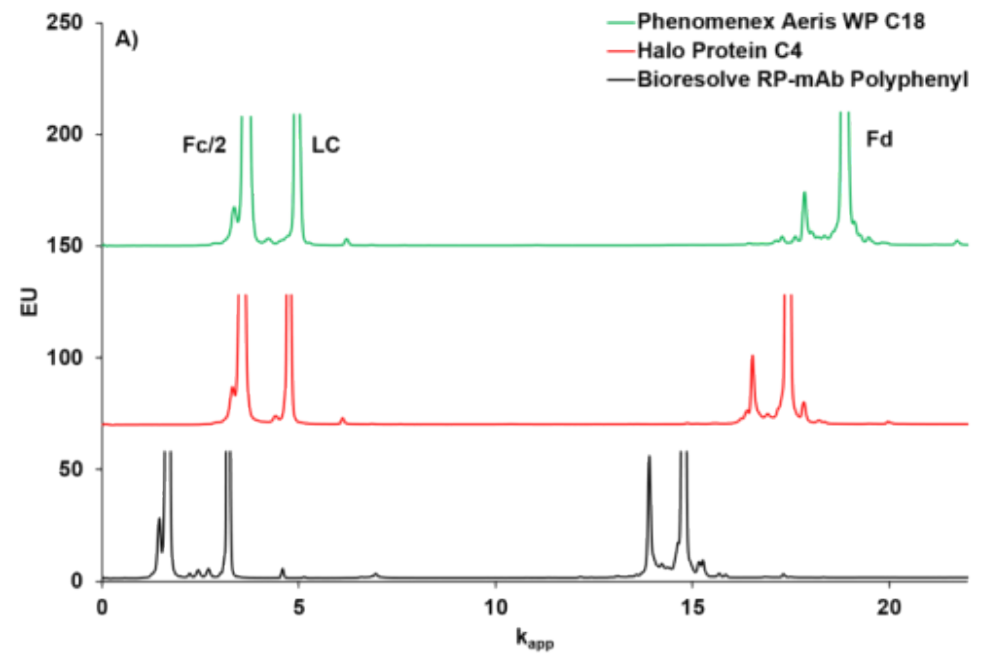


Figure 2

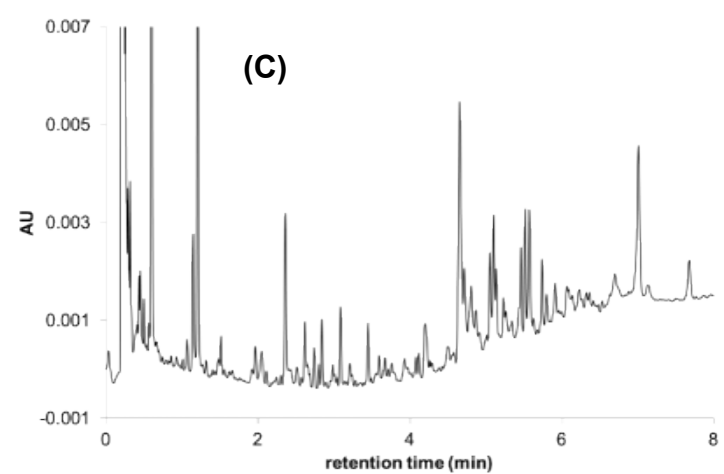
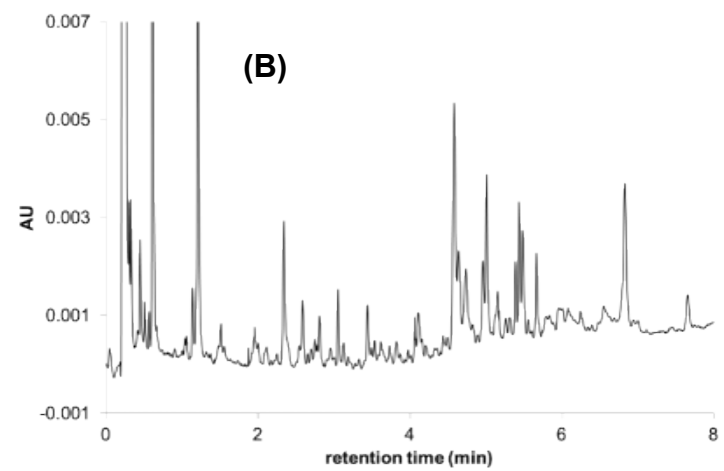
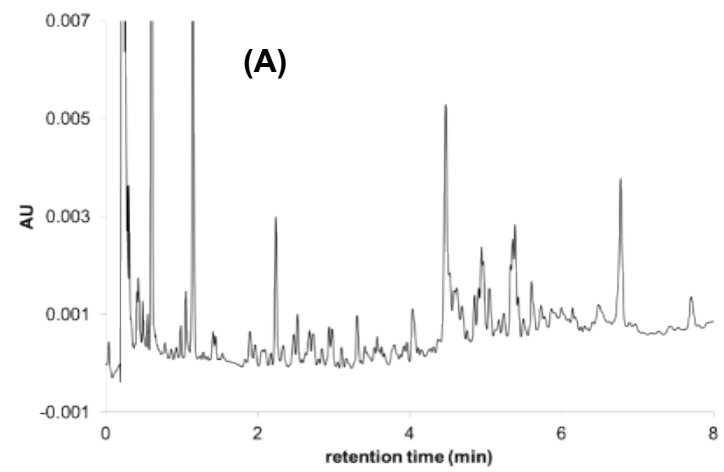


Figure 3

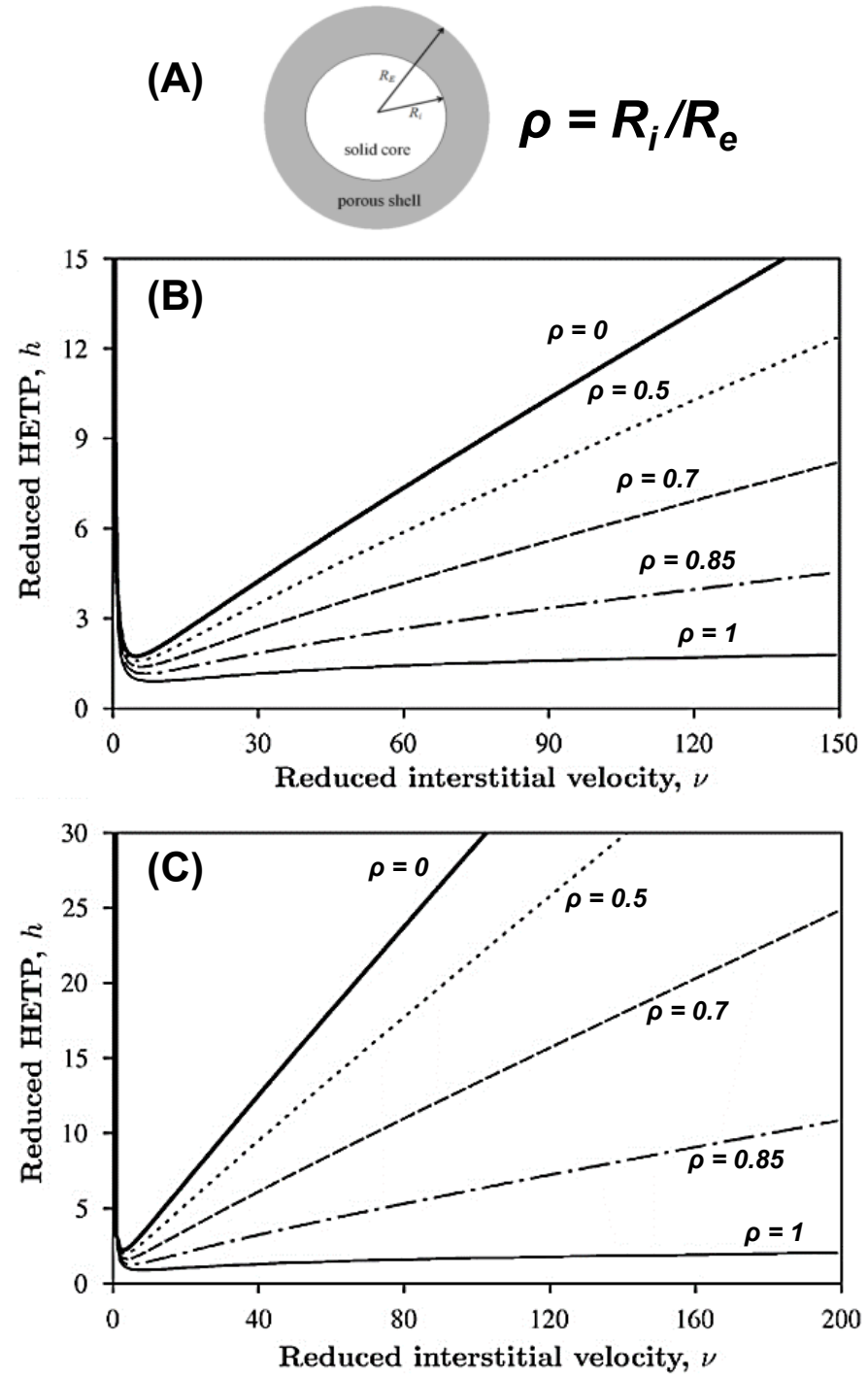


Figure 4

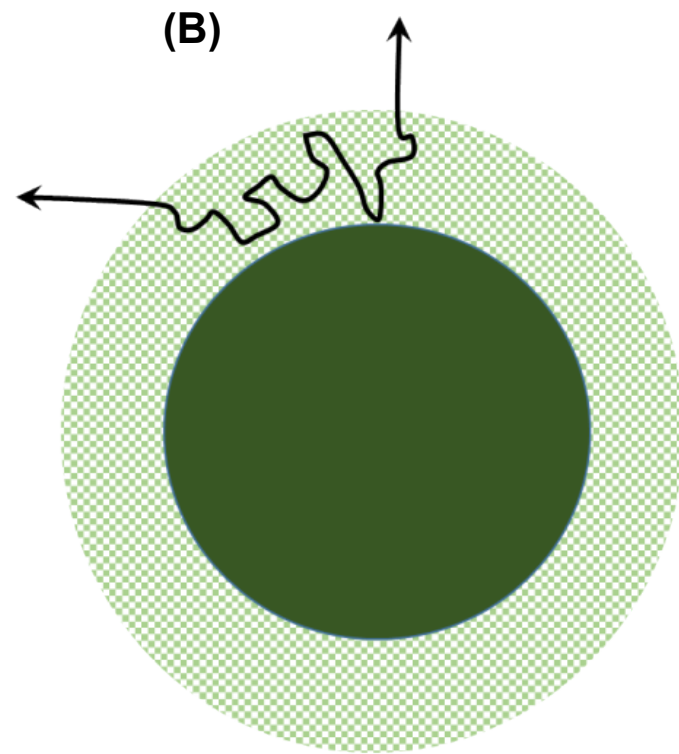
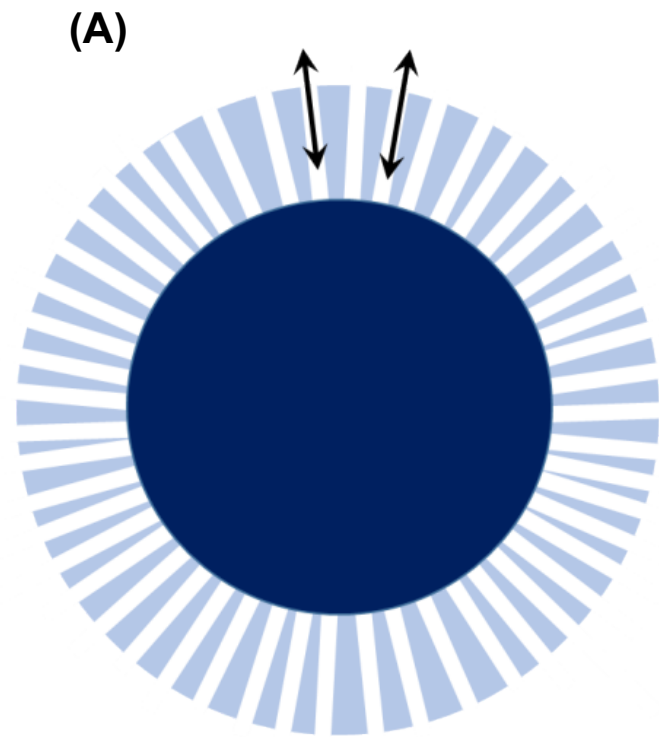


Figure 5